Scaled-down 3P-4W low-voltage distribution network for testing smart grid technologies

A.M. Gross-Muresan, F.J. Matas-Diaz, M. Barragán-Villarejo, J.M. Maza-Ortega, *Member, IEEE*, E. Romero-Ramos, *Member, IEEE*.

***Abstract*—Low-voltage distribution networks are facing nowadays a major transformation to tackle the long-awaited decarbonization of our society. This paper presents a physical scaled-down unbalanced three-phase four-wire (3P-4W) low-voltage distribution network for testing new software and hardware technologies which may foster this revolution. The aim is to develop a test bed able to faithfully reproduce the performance of this part of the power system. In this manner, it would be possible to assess the impact that any technology may have in advance to an actual field deployment. The paper describes the main design considerations for representing end users, comprising load and/or generators, and a detailed model of the unbalanced network including coupling between phases. The build scaled-down distribution network has been assessed through a comprehensive set of unitary and integrated tests which are compared to simulation results to evidence the effectiveness of its design. The paper closes with the main conclusions and an outline of the future works that can be carried out using the described test bed.**

***Index Terms*—Distribution networks, 3P-4W networks, 3P-4W VSC, unbalance network.**

I. Introduction

DISTRIBUTION networks, and particularly low-voltage (LV) ones, have been traditionally of minor significance compared to the transmission level, where large power plants are connected to supply the total power system demand. Distribution networks deliver the power to the final user but, in spite of this central role, their design and operation have remained simple. Their passive nature along with the radial topology are to a large extent the reasons for that. In fact, with appropriate planning procedures and some basic control actions in primary substations, it was possible to achieve a secure operation, i.e. nodal voltages and feeder currents within the technical limits, without any real-time supervision.

This conventional approach has dramatically changed in recent years due to a massive penetration of renewable distributed generation. Individual citizens play a major role in this process, due to climate change concerns and the recent impact of skyrocketing energy prices on the domestic economies. Furthermore, in this context the so-called smart grid technologies are ready, leveraging the transition towards a completely active network in which end-users are empowered into prosumers. This change of paradigm is a tremendous challenge since the *fit and forget* strategy has to evolve to an actual active network management.

As a result, this situation requires advanced methods with the aim of getting a deeper knowledge of the LV network to assess the impact that any new technology may have. For this purpose, accurate models reproducing the actual performance of LV distribution networks are of utmost importance. It is possible to find different approaches in the specialized literature to tackle this issue: test networks [1]- [3], representative networks [4]- [6] and even actual networks [7]. These distribution networks models have been widely used in simulation studies to analyze the impact that the new smart technologies may have.

In addition to this, a revival of physical laboratory models of different power system components have appeared in the last years. These hardware models may provide an understanding of some physical phenomena which are unnoticed on a simulation environment, providing a relevant feedback before any pilot testing on an actual system. Scaled-down laboratories, in terms of voltage and power, are the preferred solution for education and research activities within universities and research centers due to economic and safety reasons. With this regard, different experimental scaled-down transmission line test beds are presented in [8], [9] and [10] to analyze the frequency-dependant performance of this power system component. Scaled-down models of substations have also been reproduced in the laboratory to deal with automation and protection issues in this environment [11]. Regarding microgrids, [12] describes a laboratory for analyzing the mutual influence of PV inverters during islanding detection, [13] describes a setup for analyzing the interaction between two converters within a microgrid, [14] presents a power Hardware in the Loop microgrid test bed to analyze energy management tools and [15] a test bench for a more electrical aircraft application.

Distribution networks have been also reproduced in the laboratory using scaled-down representations for different purposes. Thus, the impact of power quality is analyzed in the laboratory described in [16] using a representation of the IEEE-13 node test feeder. Miniature scaled-down systems are a cost-effective solution discussed for the application of fault location algorithms [17] and arc-fault characterization [18]. A scaled-down distribution system reproducing the European

All authors are with the Department of Electrical Engineering, Universidad de Sevilla, Spain. E. Romero-Ramos is also with ENGREEN Laboratory of Engineering for Energy and Environmental Sustainability, Universidad de Sevilla, Spain.

This work was supported by Grant PID2021-124571OB-I00 funded by MCIN/AEI/ 10.13039/501100011033 and by "ERDF A way of making Europe", by the CERVERA research programme of CDTI, the Industrial and Technological Development Centre of Spain under the research Project HySGrid+ (CER-20191019), and by Grant TED2021-131604B-I00 funded by MCIN/AEI/10.13039/501100011033 and by the "European Union NextGenerationEU/PRTR".

Manuscript received July 28, 2023; revised August 26, 2023.

MV benchmark distribution network proposed by the CIGRE Task Force C6.04.02 has been presented in [19], with the aim of analyzing the impact of renewable generation in MV distribution networks. In addition to this, scaled-down distribution networks are widely used for assessing the impact of coordinated control of distributed resources [20], [21], [22] and [23].

This paper presents two major contributions with respect all these previous works, particularly [19], to consider the special features of LV networks. First, final users, either load and generators, are represented by the so-called Omnimode Load Emulators (OLEs), [19], with a three-phase four-wire (3P-4W) topology. The OLEs are voltage source converters (VSCs) equipped with a tailor-made control algorithm able to reproduce any unbalance condition. Second, a detailed distribution network model is proposed, considering the inductive coupling between the phases, which is key to faithfully reproduce the impact of load imbalance.

The paper is organized as follows. Section II briefly presents the European residential LV benchmark distribution network proposed by the CIGRE Task Force C06.04.02. Section III is devoted to provide the design procedure considered for building the scaled-down version of this network in the laboratory. This includes all the details of power converters mimicking the performance of final users, either load or generators, and the unbalance network model considering the phase couplings. Section IV describes the final realization of the scaled-down system while section V presents all the validation results related to unitary and system testing. Finally, section VI closes the paper with the main conclusions and future work.

II. Benchmark LV network

It is well known that there are two main approaches to design distribution networks, referred to as European and North American styles [24]. This paper focuses on European LV distribution systems, although its extension to North American medium voltage networks would be the next natural step in the research.

The considered benchmark network is part of the 400-V European LV reference network proposed by CIGRE [2], more specifically the residential sub-network, whose one-line diagram is shown in Fig. 1. This sub-network will henceforth be referred to as the CIGRE reference network which will be scaled-down in the laboratory.

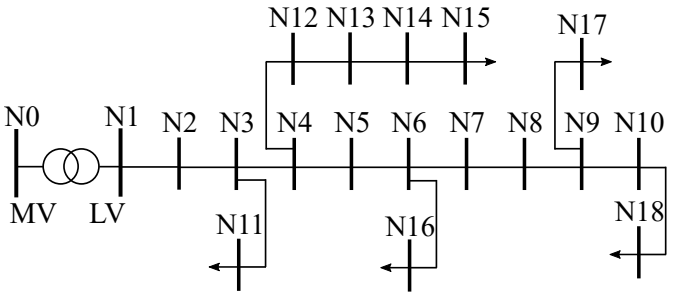

Fig. 1. Topology of residential European LV benchmark network.

This subnetwork provides connection points to both single-phase and three-phase prosumers, using 570 meters of underground 3P-4W cables fed from a 20/0.4 kV-500 kVA three-phase delta-star transformer. The grounding follows a TT scheme since it is widely used, particularly in the European networks [25].

III. Scaled-down distribution network design

The following subsections describe the main components of the scaled-down distribution network, namely: consumers/generators and line sections. Note that the secondary substation transformer has been represented by an actual device as described in section IV.

A. Consumers and distributed generators

The loads/generators connected to each node of the scaled-down LV network are emulated through the so-called OLEs. As previously mentioned an OLE is a 3P-4W VSC with an LCL coupling filter as shown in Fig. 2. These devices can inject/absorb any active and reactive power according to the user needs, mimicking final users with loads and/or generators. According to Fig. 1, at least five OLEs rated to 400 V and 20 kVA are connected in leaf nodes in the scaled-down network.

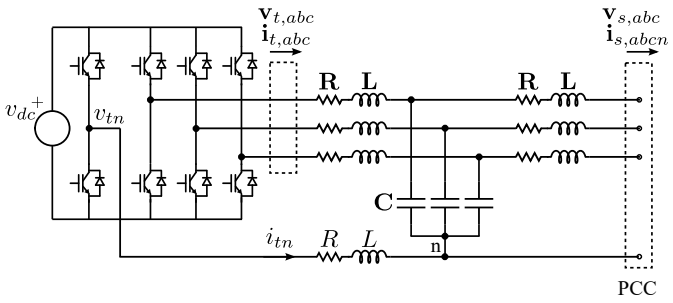

Fig. 2. 3P-4W OLE with an LCL coupling filter for emulation of prosumers in the scaled-down LV network.

These OLEs must impose different active and reactive power injections per phase to properly represent the load imbalance. Note that the 3P-4W OLEs are controlled as current sources and, therefore, adequate current references are required. In case of balance conditions, these current references are set in a straightforward manner from the active and reactive power references either in the $\alpha\beta$ or dq domains using an instantaneous power formulation [19]. This is not the case, however, for unbalanced loads since the instantaneous three-phase powers contain both constant and oscillating 100 Hz terms. Therefore, it is difficult to establish a mapping between the reference phase powers and the corresponding instantaneous power components required for the OLE current control. Appendix A outlines a discussion of power theory in unbalanced three-phase systems to clarify the definition of steady-state and instantaneous powers.

For this reason, it is proposed to apply a control algorithm with an independent power control per phase. The proposed control strategy is based on the assumption that the 3P-4W OLE can be controlled as three independent single-phase

devices, one per phase, with independent active and reactive power references. For doing so, it is proposed to generate a virtual three-phase system related to each phase of the 3P-4W OLE to take advantage of this characteristic of the balanced systems. To do this, the phase m voltage is associated with the α component of its virtual $\alpha\beta$ stationary frame, while its counterpart β component is obtained by delaying the α signal $\pi/2$ radians. This delay can be achieved in different ways [32], particularly this work has applied two cascaded low-pass filters tuned to the fundamental frequency ω:

$$v_{m,\alpha} = v_m \qquad v_{m,\beta} = 2 \cdot \frac{\omega}{s+\omega} \cdot \frac{\omega}{s+\omega} v_{m,\alpha}. \tag{1}$$

Note that these $v_{m,\alpha}$ and $v_{m,\beta}$ have the same amplitude with a delay of $\pi/2$ radians which corresponds to a balanced three-phase system.

In this virtual three-phase framework of phase m, $3P^\star_m$ and $3Q^\star_m$ are the three-phase power references, being the current setpoints $i^\star_{m,\alpha}$ and $i^\star_{m,\beta}$ defined as:

$$i^\star_{m,\alpha} = 2\frac{P^\star_m v_{m,\alpha} - Q^\star_m v_{m,\beta}}{v^2_{m,\alpha} + v^2_{m,\beta}} \; i^\star_{m,\beta} = 2\frac{P^\star_m v_{m,\beta} - Q^\star_m v_{m,\alpha}}{v^2_{m,\alpha} + v^2_{m,\beta}} \tag{2}$$

Once these virtual references of phase m have been computed, it is required to undo the change returning to the real system. For doing so, the virtual α component is associated with the reference current of its corresponding phase:

$$i^\star_a = i^\star_{a,\alpha} \quad i^\star_b = i^\star_{b,\alpha} \quad i^\star_c = i^\star_{c,\alpha} \tag{3}$$

and the neutral current is computed as:

$$i^\star_n = -\left(i^\star_a + i^\star_b + i^\star_c\right). \tag{4}$$

The above equations provide the real system reference currents in the phase domain which can be converted to the $\gamma\alpha\beta$ domain to perform the current tracking by means of resonant controllers. Fig. 3 shows the proposed strategy for independent power control per phase.

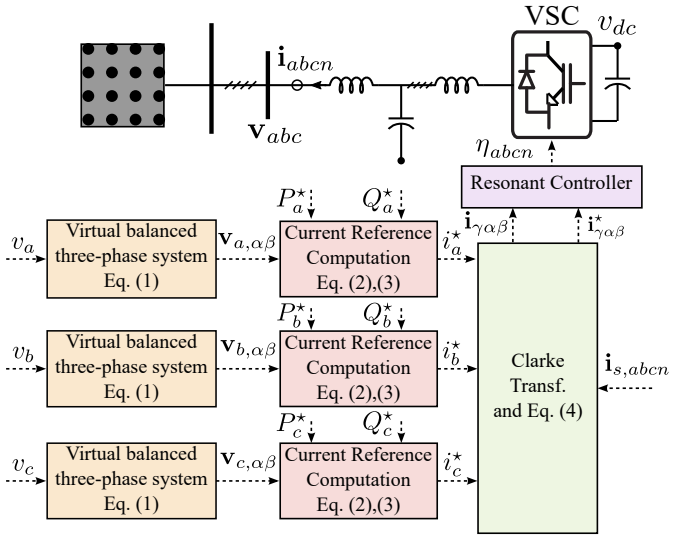

Fig. 3. Proposed strategy for independent power control per phase in OLE.

B. Power lines

Fig. 4 shows the steady-state phase-domain model representing a 3P-4W line section of extremes i and j. Note that shunt admittances are ignored because of the short length of LV lines, and only the resistance of the conductors and the self and mutual inductive impedances among phases are considered [29]. This model drives to a 4×4 series impedance matrix that allows to obtain (5) after applying Kirchhoffs' voltage law to the circuit of Fig. 4.

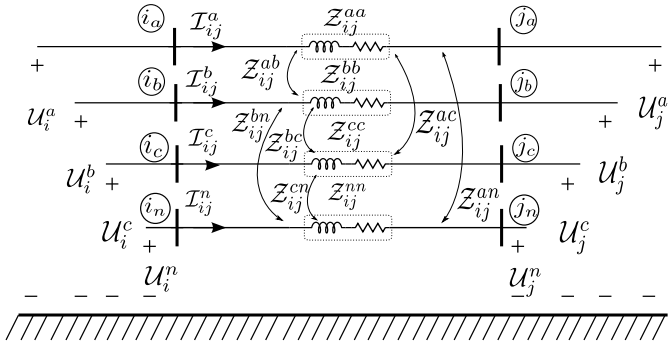

Fig. 4. 3P-4W line section model.

$$\begin{bmatrix}\mathcal{U}^a_i\\ \mathcal{U}^b_i\\ \mathcal{U}^c_i\\ \mathcal{U}^n_i\end{bmatrix} - \begin{bmatrix}\mathcal{U}^a_j\\ \mathcal{U}^b_j\\ \mathcal{U}^c_j\\ \mathcal{U}^n_j\end{bmatrix} = \begin{bmatrix}\mathcal{Z}^{aa}_{ij} & \mathcal{Z}^{ab}_{ij} & \mathcal{Z}^{ac}_{ij} & \mathcal{Z}^{an}_{ij}\\ \mathcal{Z}^{ab}_{ij} & \mathcal{Z}^{bb}_{ij} & \mathcal{Z}^{bc}_{ij} & \mathcal{Z}^{bn}_{ij}\\ \mathcal{Z}^{ac}_{ij} & \mathcal{Z}^{bc}_{ij} & \mathcal{Z}^{cc}_{ij} & \mathcal{Z}^{cn}_{ij}\\ \mathcal{Z}^{an}_{ij} & \mathcal{Z}^{bn}_{ij} & \mathcal{Z}^{cn}_{ij} & \mathcal{Z}^{nn}_{ij}\end{bmatrix}\begin{bmatrix}\mathcal{I}^a_{ij}\\ \mathcal{I}^b_{ij}\\ \mathcal{I}^c_{ij}\\ \mathcal{I}^n_{ij}\end{bmatrix}. \tag{5}$$

Based on this model, next simplifications are commonly adopted:

- If a perfect multi-grounded neutral is assumed, and the Kron reduction is applied because of $\mathcal{U}^n_i$ and $\mathcal{U}^n_j$ are zero, the original 4×4 series impedance matrix is reduced to a 3×3 phase frame matrix. The worse the grounding, i.e. the higher the value of the grounding resistance, the larger the error that will be made with this simplification [30].
- It is quite common among utilities to only have the positive sequence impedance of the lines available, what drives to a 3×3 diagonal phase matrix, or even a 4×4 diagonal matrix that retains neutral wire if zero impedance sequence is roughly estimated. Any of these decoupled models can lead to significant errors, mainly when imbalances in demand/generation scenarios are noticeable [30], [31].

None of these simplifications are assumed throughout this paper. On the contrary, the scaled-down system is intended to reproduce as much as possible the model posed by (5). This includes retaining the neutral conductor as well as the coupling among phases. With this purpose, (5) is modified by adding and subtracting the term $(\mathcal{Z}^{qq}_{ij} - \mathcal{Z}^m_{ij})\mathcal{I}^q_{ij}$ to each q phase equation $(q = a, b, c, n)$, where $\mathcal{Z}^m_{ij} = \sum_{p,q;p\neq q} \mathcal{Z}^{pq}_{ij}/6$, resulting (6):

$$\begin{bmatrix}\mathcal{U}^a_{ij}\\ \mathcal{U}^b_{ij}\\ \mathcal{U}^c_{ij}\\ \mathcal{U}^n_{ij}\end{bmatrix} = \begin{bmatrix}\mathcal{Z}^{aa}_{ij} - \mathcal{Z}^m_{ij} & 0 & 0 & 0\\ 0 & \mathcal{Z}^{bb}_{ij} - \mathcal{Z}^m_{ij} & 0 & 0\\ 0 & 0 & \mathcal{Z}^{cc}_{ij} - \mathcal{Z}^m_{ij} & 0\\ 0 & 0 & 0 & \mathcal{Z}^{nn}_{ij} - \mathcal{Z}^m_{ij}\end{bmatrix}\begin{bmatrix}\mathcal{I}^a_{ij}\\ \mathcal{I}^b_{ij}\\ \mathcal{I}^c_{ij}\\ \mathcal{I}^n_{ij}\end{bmatrix} + \begin{bmatrix}\mathcal{CDVS}^a_{ij}\\ \mathcal{CDVS}^b_{ij}\\ \mathcal{CDVS}^c_{ij}\\ \mathcal{CDVS}^n_{ij}\end{bmatrix} \tag{6}$$

where $\mathcal{U}_{ij}^{q} = \mathcal{U}_{i}^{q} - \mathcal{U}_{j}^{q}$ and

$$\begin{bmatrix} \mathcal{CDVS}_{ij}^{a} \\ \mathcal{CDVS}_{ij}^{b} \\ \mathcal{CDVS}_{ij}^{c} \\ \mathcal{CDVS}_{ij}^{n} \end{bmatrix} = \begin{bmatrix} \mathcal{Z}_{ij}^{m} & \mathcal{Z}_{ij}^{ab} & \mathcal{Z}_{ij}^{ac} & \mathcal{Z}_{ij}^{an} \\ \mathcal{Z}_{ij}^{ab} & \mathcal{Z}_{ij}^{m} & \mathcal{Z}_{ij}^{bc} & \mathcal{Z}_{ij}^{bn} \\ \mathcal{Z}_{ij}^{ac} & \mathcal{Z}_{ij}^{bc} & \mathcal{Z}_{ij}^{m} & \mathcal{Z}_{ij}^{cn} \\ \mathcal{Z}_{ij}^{an} & \mathcal{Z}_{ij}^{bn} & \mathcal{Z}_{ij}^{cn} & \mathcal{Z}_{ij}^{m} \end{bmatrix} \begin{bmatrix} \mathcal{I}_{ij}^{a} \\ \mathcal{I}_{ij}^{b} \\ \mathcal{I}_{ij}^{c} \\ \mathcal{I}_{ij}^{n} \end{bmatrix}$$

are current-controlled voltage sources, what allows representing (6) by the equivalent circuit shown in Fig. 5.(a). These dependent voltage sources in series with the impedance $(\mathcal{Z}_{ij}^{qq} - \mathcal{Z}_{ij}^{m})$ at each phase can be transformed into dependent current sources $\mathcal{CDCS}_{ij}^{q} = \dfrac{\mathcal{CDVS}_{ij}^{q}}{(\mathcal{Z}_{ij}^{qq} - \mathcal{Z}_{ij}^{m})}$ in parallel with the same impedance, what is illustrated in Fig. 5.(b). Finally, each of the three dependent current sources at phases a, b and c are shifted as shown in Fig. 5.(c), where it can be easily checked how Kirchhoffs' current law remains unchanged at each node of the circuit.

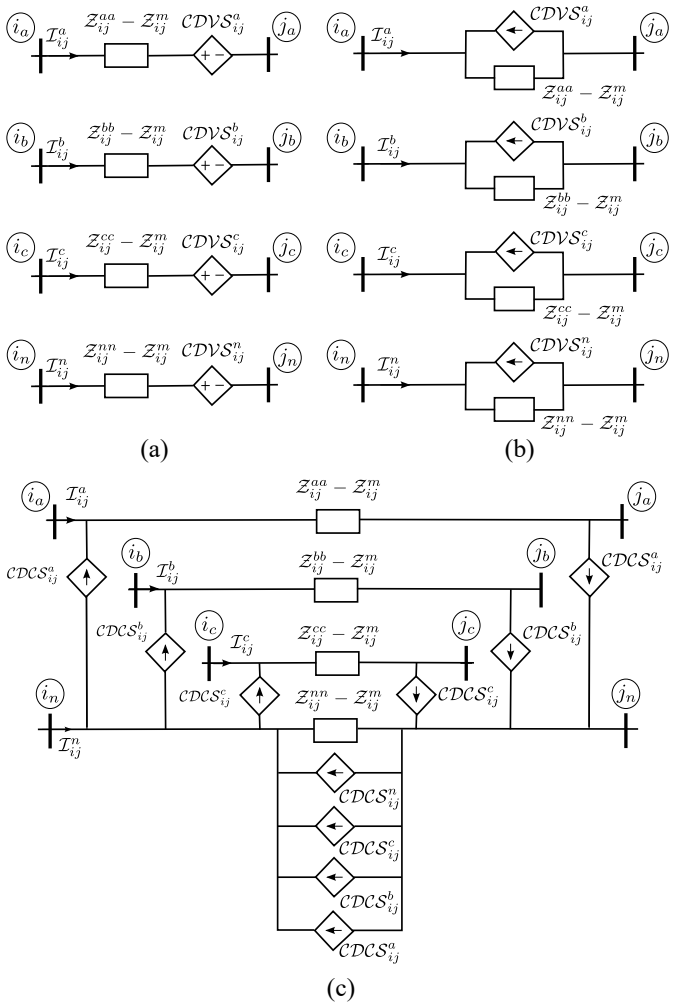

Fig. 5. Transformation of the 3P-4W line model. (a) Controlled voltage source; (b) Controlled current source; (c) Shifting of current sources.

As for the total dependent current source between the two extremes of the neutral conductor, (7) results after grouping together all the terms that multiply each current:

$$\sum_{q=a,b,c,n} \mathcal{CDCS}_{ij}^{q} = \mathcal{K}_{ij}^{a}\mathcal{I}_{ij}^{a} + \mathcal{K}_{ij}^{b}\mathcal{I}_{ij}^{b} + \mathcal{K}_{ij}^{c}\mathcal{I}_{ij}^{c} + \mathcal{K}_{ij}^{n}\mathcal{I}_{ij}^{n} \quad (7)$$

where,

$$\mathcal{K}_{ij}^{q} = \frac{(\mathcal{Z}_{ij}^{m} + \sum_{p,p\neq q} \mathcal{Z}_{ij}^{qp})}{(\mathcal{Z}_{ij}^{qq} - \mathcal{Z}_{ij}^{m})} \quad \forall \quad q = a, b, c, n$$

These coefficients $\mathcal{K}_{ij}^{q}$ are identical when the same type of conductor is used for each phase and the neutral, even if the geometrical arrangement of the power line is symmetrical/transposed or even quasi-symmetrical. The first condition is quite common, although it is also frequent to choose a conductor of a smaller gauge for the neutral. On the other hand, the condition of structural balance is more unusual, but since the distances between phases are smaller at these LV levels the result is that the couplings between phases are practically of the same order. Table I illustrates the values $\mathcal{K}_{ij}^{q}$ for the different types of 3P-4W line cross-sections proposed by CIGRE in [2] for the European LV benchmark network.

TABLE I
$\mathcal{K}_{ij}^{q}$ VALUES FOR DIFFERENT LINES OF CIGRE EUROPEAN LV BECHMARK NETWORK.

Type of line	$\mathcal{K}_{ij}^{a}$	$\mathcal{K}_{ij}^{b}$	$\mathcal{K}_{ij}^{c}$	$\mathcal{K}_{ij}^{n}$
UG1	7,557 +12,642j	7,557 +12,642j	7,557 +12,642j	7,557 +12,642j
UG2	3,581 + 9,146j	3,581 + 9,146j	3,581 + 9,146j	3,581 + 9,146j
UG3	0,592 + 3,402j	0,592 + 3,402j	0,592 + 3,402j	0,592 + 3,402j
OH1	1,992 + 2,625j	2,054 + 2,728j	2,054 + 2,728j	1,992 + 2,625j
OH2	0,478 + 1,305j	0,490 + 1,355j	0,490 + 1,355j	0,478 + 1,305j
OH3	0,250 + 0,891j	0,256 + 0,924j	0,256 + 0,924j	0,250 + 0,891j

Note that the near-equality between the coefficients $\mathcal{K}_{ij}^{q}$, and the fact that the sum of the currents through the four wires of the line is zero because of the isolated neutral condition, lead to the cancellation of (7). This result finally implies that it is possible to represent the coupling among conductors by two equal and opposite current dependent current sources connected to both ends of each phase, as schemed in Fig. 6.

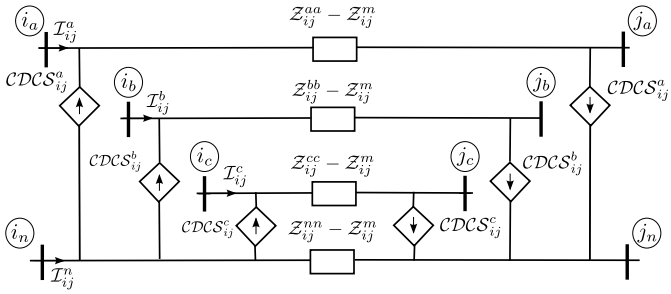

Fig. 6. Proposed three-phase four-wire line model.

Observe that if the 3P-4W line were transposed, $\mathcal{Z}_{ij}^{m}$ would represent the single common coupling among phases, and (5) would drive to a full decoupled model with each phase q exactly modelled by the series impedance $(\mathcal{Z}_{ij}^{qq} - \mathcal{Z}_{ij}^{m})$ because of the isolated neutral. This ideal case is also fulfilled in the proposed model by making the dependent sources null, which leads to the understanding that the dependent sources $\mathcal{CDCS}_{p}$ model the asymmetry of the power line.

This transformation allows to represent the unbalanced coupling between the phases by proper current injections that

can be emulated in the laboratory using OLEs. Basically, these currents are added to the reference currents computed for the load/generation emulation of Fig. 3. In this way, the two functions can be carried out simultaneously by the OLEs: load emulation and phase coupling.

IV. Scaled-down LV network test bed

The residential CIGRE European LV benchmark system in Fig. 1 is reduced to the 12-bus network shown in Fig. 7, where those series line sections with the same conductor have being grouped together. Note that this simplification just affect to the network branches since the nodes with loads/generators remain unaltered. Table II lists the series impedance $(\mathcal{Z}_{ij}^{p} - \mathcal{Z}_{ij}^{m})$ for each line ij obtained as described in section III and using the information provided in [2]. The same series impedance results for any of the phases and neutral because both type of underground cables UG1 and UG3 use the same conductor section for all the wires. These impedances are the theoretical ones to be reproduced in the laboratory.

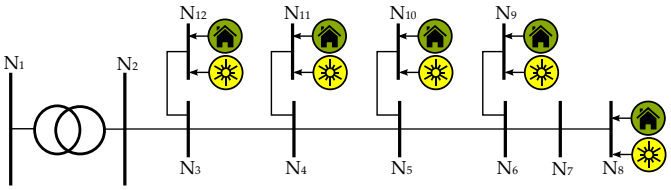

Fig. 7. One-line diagram of the scaled-down LV network.

TABLE II
Line data for the reduced CIGRE LV European benchmark network of Fig. 7

Node from	Node to	$(\mathcal{Z}_{ij}^{p} - \mathcal{Z}_{ij}^{m})$ [Ω]	Length [m]
2	3	$0.0113 + j0.0057$	70
3	4	$0.0057 + j0.0028$	35
4	5	$0.0113 + j0.0057$	70
5	6	$0.0170 + j0.0085$	105
6	7	$0.0057 + j0.0028$	35
7	8	$0.0247 + j0.0026$	30
6	9	$0.0247 + j0.0026$	30
5	10	$0.0247 + j0.0026$	30
4	11	$0.0863 + j0.0090$	105
3	12	$0.0247 + j0.0026$	30

The scaled-down version of this actual network is done by applying a change in the base magnitudes. For doing so, it has to be considered the ratings of the devices available in the laboratory. On the one hand, the rated voltage is set to 400 V. On the other hand, the rated power has been scaled-down 6 times due to the power limitations of the OLEs. Furthermore, the commercial resistors and reactors available in the market to reproduce the series impedance are different from these theoretical values, resulting those shown in Table III. It is worth noting that the resistive part of the reactors contributes to the total resistance of the line sections. As a result, the length of each individual line sections increases as specified in Table III. In addition, the final reactor values force to recompute the distances among phases, these changing from the original 1.75 cm and 0.8 cm specified in [2] for UG1 and UG3 respectively, to new values ranging from 1.3 cm to 4.7 cm, all of them very realistic. These readjustments allow to accurately model the network finally available in the laboratory. This exact model will be used in steady-state analysis to compare the theoretical simulated results with experimental ones.

TABLE III
Line data for the actual laboratory scaled-down network of Fig. 7

Node from	Node to	$(\mathcal{Z}_{ij}^{p} - \mathcal{Z}_{ij}^{m})$ [Ω]	Length [m]
2	3	$0.1040 + j0.0623$	107
3	4	$0.0464 + j0.0300$	47.7
4	5	$0.0900 + j0.0572$	92.6
5	6	$0.1415 + j0.1117$	145.6
6	7	$0.0437 + j0.0359$	45
7	8	$0.1792 + j0.0278$	36.3
6	9	$0.1773 + j0.0239$	36
5	10	$0.1719 + j0.0214$	34.8
4	11	$0.5169 + j0.0793$	104.8
3	12	$0.1756 + j0.0243$	40.1

Regarding the OLEs, those available in lab have a rated power of 20 kVA. The energy absorbed/injected by the OLEs is managed through a multiterminal DC-link identical to the proposal of [19], where an extra balancing VSC is in charge of controlling the common DC bus voltage and providing the net power required by all OLEs.

Finally, a three-phase delta-star 400/400 V 125 kVA transformer with a short-circuit impedance of $0.0166 + j0.0227$ p.u. is at the head of the feeder, being energized by a 100 kVA power supply. Fig. 8 shows the layout of the whole scaled-down LV network with indication of its main components.

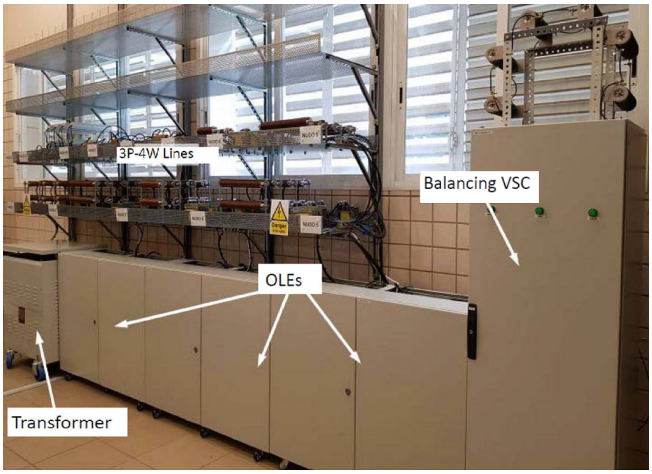

Fig. 8. Physical appearance of the scaled-down 3P-4W LV network.

V. Validation of the scaled-down network

This section presents some experimental tests to evidence the accuracy of the built scaled-down distribution network. For doing so, the experimental results are compared with simulations done over the modified CIGRE network whose parameters are depicted in Table III. Two types of tests have been performed; (i) unitary tests to validate the individual performance of the main network components; (ii) integrated

tests with realistic daily load/generation curves to analyze the impact on the voltage profiles.

A. Unitary testing

Two group of tests have been carried out within this subsection. The first one consists of validating the OLE independent power control per phase presented in section III-A, which makes it possible to represent the unbalanced loads/generators. While the second set of tests evaluate the performance of the scaled-down network for different operating points considering or disregarding the coupling between phases as proposed in section III-B.

1) OLE Independent power control per phase: In this test, the OLE is directly connected to a controllable AC voltage source which sets a balanced 50 Hz, 230 V phase-to-neutral voltage. Initially, the OLE is operating in a balanced manner with 3 kW and 0 kvar as power references per phase. In order to evaluate the performance of the controller, a step change in the active power reference $P_c^\star$ is produced at $t = 0.06$ s. Fig. 9 shows the phase and neutral currents and the corresponding active and reactive phase powers. At the beginning, the currents are balanced and the phase active and reactive powers are equal as expected. Note that the power reference change of phase c from 3 kW to 4 kW turns the currents unbalanced. In fact, the neutral current is no longer zero. The performance of the controller is good both from a steady-state and dynamic points of view. In any case, the total harmonic distortion (THD) of the injected currents is below 1.33 % and 1.46% in the balanced and unbalanced scenarios respectively. Moreover, the controller is able to track the reference change achieved in less than one cycle as shown in the top plot of Fig. 9. Finally, note that the phase powers shown in the bottom plot of Fig. 9 have been obtained applying a low-pass filter to their corresponding instantaneous value to remove the oscillating 100 Hz term. This causes a slower dynamics in the shown time evolution.

2) Unbalance LV network model: This group of tests has two main objectives: (i) to represent the couplings of the power lines with the methodology proposed in subsection III-B; (ii) to evaluate the accuracy of the scaled-down system by comparing experimental and simulation results obtained from a power flow analysis.

Since the objective of these unitary tests is to validate the proposed coupled network model, the transformer connected between nodes N1 and N2 has been removed. The node N2 is directly supplied by a controllable AC source that maintains a balanced 400 V and 50 Hz voltage. In addition, a relative high load is connected to node N7 to cause a significant voltage variation with respect to the node N2. Several tests with balanced and unbalanced reference powers and unitary, inductive and capacitive power factors, all of them detailed in Table IV, are commanded to the OLE in N7 in order to cover a wide range of operating points. The emulation or omission of the coupling between phases using OLEs is also compared. Note as cases I and II are balanced load scenarios while cases III and IV are unbalanced. Table IV also shows the phase-neutral voltages at node N7 obtained in both experimental and simulation tests, considering or dismissing the coupling in lines.

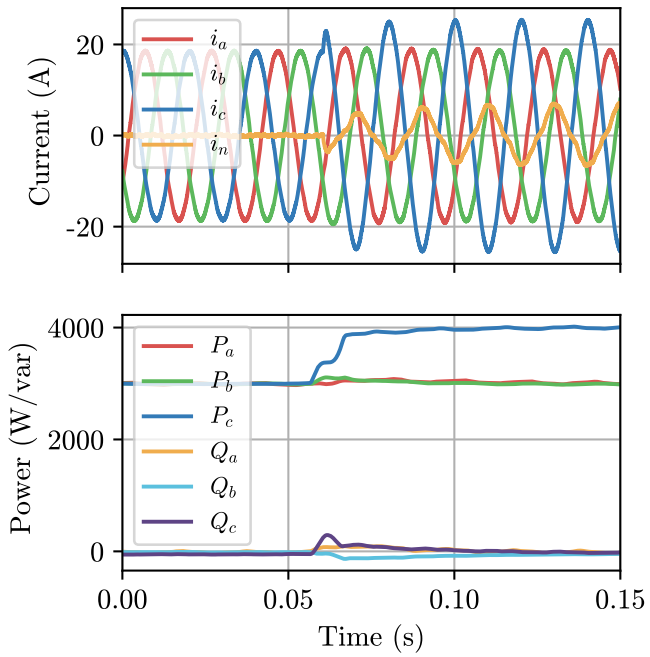

Fig. 9. Step reference change of $P_c^\star$ for evaluation of the OLE independent power control per phase. Top plot: Instantaneous $abcn$ currents. Bottom plot: Filtered active and reactive power per phase.

The balanced decoupled experimental tests, Case I and II, show a slight unbalance between the phase voltages, which is due to the differences between the parameters of the power lines of each phase in the lab. Note that although the resistance and inductance of the phases are theoretically identical ($\mathcal{Z}_{ij}^{qq} - \mathcal{Z}_{ij}^{m}$), practical network installation issues such as electrical connections, connection cables between elements, tolerance of the elements, etc. lead to this small difference between the three phases. These practical issues also affect the mismatch between experimental and simulation results. As can be seen, the simulation results of Cases I and II keep the voltages balanced for the decoupled tests as expected, since the parameters per phase are identical in this environment. In addition, their values are slightly higher than the experimental ones. The effect of reactive power in the network voltages is reflected in Case II with respect to Case I for the decoupled tests. It is observed that the voltages of Case II are lower than Case I due to the consumption of reactive power, although the apparent power demanded by the OLE is identical in both cases.

For the coupled tests of Cases I and II, an expected variation among the three phase voltages is observed compared to the decoupled tests, both for experimental and simulation results. To evaluate the effect of the phase coupling, an error ϵ is calculated between the voltages of the coupled and decoupled tests. This parameter indicates that in balanced situations, whether or not the coupling is taken into account leads to a voltage error of about 1% in some phases of the system, such as the voltage V_a in Cases I and II. In addition, it is observed that the

TABLE IV
UNITARY TESTS. LOAD SCENARIOS, SIMULATED AND EXPERIMENTAL PER UNIT VOLTAGES AT N7 WITH AND WITHOUT CONSIDERING THE PHASE COUPLING.

Case	Load scenarios				Experimental Results				Simulated Results		
	P (kW)	Q (kvar)	S (kVA)	Power factor	Voltage	Decoup.	Coup.	ε (%)	Decoup.	Coup.	ε (%)
I	5	0	5	1	V_a	0.9500	0.9419	−0.87	0.9576	0.9468	−1.14
	5	0	5	1	V_b	0.9498	0.9493	−0.05	0.9576	0.9579	0.03
	5	0	5	1	V_c	0.9474	0.9561	0.90	0.9576	0.9682	1.11
	P (kW)	Q (kvar)	S (kVA)	Power factor	Voltage	Decoup.	Coup.	ε (%)	Decoup.	Coup.	ε (%)
II	4	3	5	0.8 (lag)	V_a	0.9415	0.9315	−1.07	0.9484	0.9406	−0.83
	4	3	5	0.8 (lag)	V_b	0.9411	0.9368	−0.46	0.9484	0.9463	−0.22
	4	3	5	0.8 (lag)	V_c	0.9401	0.9449	0.50	0.9484	0.9583	1.04
	P (kW)	Q (kvar)	S (kVA)	Power factor	Voltage	Decoup.	Coup.	ε (%)	Decoup.	Coup.	ε (%)
III	9	0	9	1	V_a	0.8408	0.8386	−0.26	0.8330	0.8283	−0.57
	4.5	0	4.5	1	V_b	1.0030	1.0095	0.64	1.0180	1.0253	0.70
	1.5	0	1.5	1	V_c	1.0088	1.0187	0.98	1.0170	1.0315	1.41
	P (kW)	Q (kvar)	S (kVA)	Power factor	Voltage	Decoup.	Coup.	ε (%)	Decoup.	Coup.	ε (%)
IV	7.2	-5.4	9	0.8 (lead)	V_a	0.9043	0.9008	−0.38	0.9112	0.9030	−0.90
	3.6	-2.7	4.5	0.8 (lead)	V_b	1.0428	1.0484	0.54	1.0570	1.0643	0.69
	1.2	-0.9	1.5	0.8 (lead)	V_c	0.9790	0.9911	1.22	0.9825	0.9971	1.47

emulation of the coupling in the experimental case by the OLE yields to ϵ values in the same order of magnitude and tendency as those obtained in the simulation tests. The slight differences in the errors obtained from experimental and simulation tests are mainly due, once again, to the aforementioned mismatch between the phase parameters of the power lines.

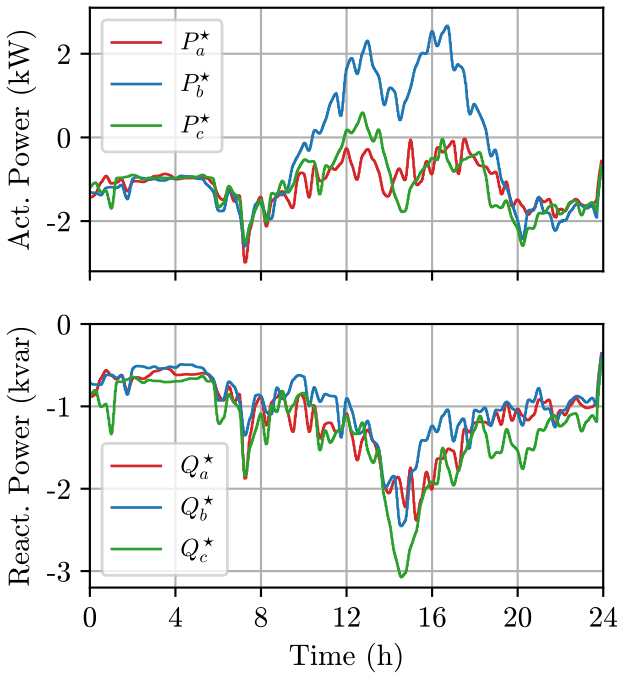

Fig. 10. 24-hour net active and reactive power profiles per phase of all the generators and loads.

For the unbalanced load tests, Cases III and IV, a large variation of the phase voltages is observed in the decoupled tests, especially V_a with respect to the other two phases, since it is the phase with the highest percentage of load. Note that V_b and V_c are even greater than 1 p.u. in case III and despite the fact that they represent a consumption, due to the load imbalance. In a similar way to the balanced cases I and II, the voltages between the experimental and the simulation results are aligned, once again existing a slight difference because the line parameters in the experimental and simulation tests are not identical. The effect of reactive power is observed in the voltages of case IV with respect to those of case III, resulting in a general voltage increase caused by the reactive power injection of the OLE in node N7, except for phase c; this apparently non-evident voltage reduction is because of the current coming back through the neutral wire due to the load imbalance.

The emulation of the coupling in the unbalanced cases causes greater voltage differences with respect to the decoupled tests as shown in Table IV. This is reflected in an increase of ϵ which reaches values close to 1.5% in some phases. It has to be stressed that these larger errors are linked to the lightly load phases which is due to the phase coupling. In general, disregarding couplings may result in the non-detection of overvoltages/undervoltages in certain scenarios of very high load or high penetration of renewables [33]. Finally, the trend of ϵ for each phase using experimental and simulation results is coherent.

B. Integrated testing

This test consists of evaluating the overall performance of the scaled-down distribution network, representing the unbalanced load conditions and phase coupling of LV networks. For this purpose, all the OLEs are operational and connected to their respective buses according to the one-line diagram of Fig. 7. Note that the OLEs are emulating the daily load curves of loads/generators and the phase coupling of the different branches as explained in section III.B.

The total net power profiles of all the OLEs in the system are shown in Fig. 10. These agregated profiles have been obtained in a synthetic manner from smart meter data of

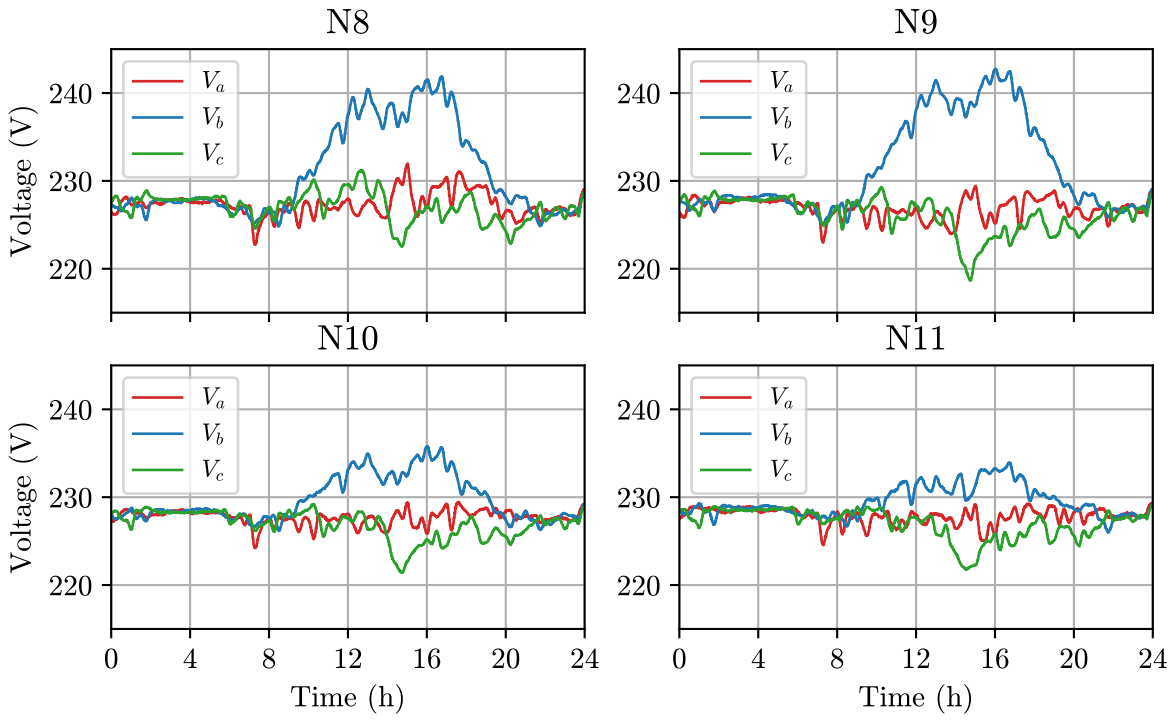

Fig. 11. 24-hour profiles of the nodal voltages at node N8, N9, N10, N11 for the test of subsection V-B.

individual Spanish final users, with loads and PV generation, in a residential area.

Most of the PV generation has been connected to phase b while most of consumers are evenly connected to phases a and c, looking for defining a 24-hour scenario with significant imbalances, as shown in Fig. 10. PV works at unity power factor, while loads operate with usual inductive power factors. These power profiles evidence the capability of the OLEs either to inject or absorb active/reactive power to represent loads or generators. Moreover, thanks to the independent power control per phase, an OLE can behave as both load and generator in different phases simultaneously. The 24-hour profiles are also scaled to 600 seconds to accommodate laboratory testing, however, they are represented in Fig. 10 in the 24-hour scale

Fig. 11 represents the nodal voltages using the previous power profiles. It is observed that the greatest voltage deviations occur in the central hours of the day when the PV generation is peaking. Of particular relevance is the voltage difference between phases b and c of the end nodes of the network, N8 and N9, which at times reaches values of up to 20 volts due to the unbalance accumulated in the whole network. This circumstance can result in simultaneous undervoltage in one phase and overvoltage in another phase, highlighting the complexity of LV networks in scenarios with high penetration of renewable energies. The voltage profiles in other intermediate nodes of the LV network, N10 and N11, follows a similar trend but with a less significant voltage increase.

VI. Conclusion

ESTHER Throughout this work, a new design solution has been proposed to replicate a 3P-4W LV network in the laboratory. This solution allows emulating both unbalanced loads and distributed generation, as well as phase couplings in network lines, the latter being of relevance in cases with significant unbalances among others. The proposed solution is largely based on the use of the OLEs, i.e. VSCs which emulate loads/generators with a per phase power control. Additionally, common circuit theory techniques have proven to be very useful to model the couplings between phases. Regarding this last contribution, it is worth mentioning that the proposed design solution allows to model couplings for both underground and overhead LV lines, making it a general purpose design proposal.

Different tests have been presented to quantify the accuracy and performance of the physical scaled-down 3P-4W network built in the laboratory, demonstrating that unbalanced scenarios have been reproduced with a high degree of fidelity and despite the limitations of working in such an environment.

This test bed promises to be the ideal framework to validate LV distribution network technologies for operation and control prior to their installation in the field. With this regard, future work will focus on the development of Advanced Demand Management System (ADMS) tools that will provide the network with the appropriate framework for its automatic management, as well as the connection of cutting-edge power devices as energy storage systems and transformers with on-load tap changers that would provide greater flexibility to the LV distribution systems.

APPENDIX A
POWER THEORY FOR UNBALANCE SYSTEMS

Let's define the instantaneous active and reactive power, $p(t)$ and $q(t)$ respectively, of a three-phase systems formulated in the phase domain as [27]:

$$p(t) = \vec{v}_{abc}(t) \cdot \vec{i}_{abc}(t)^T = p_a(t) + p_b(t) + p_c(t), \quad (8)$$

$$q(t) = \vec{v}^{\perp}_{abc}(t) \cdot \vec{i}_{abc}(t)^T = q_a(t) + q_b(t) + q_c(t), \quad (9)$$

where $\vec{v}_{abc}(t) = [v_a(t), v_b(t), v_c(t)]$ is the vector of phase voltages with respect to the neutral wire, $\vec{i}_{abc}(t) = [i_a(t), i_b(t), i_c(t)]$ is the vector of phase currents and $\vec{v}^{\perp}_{abc}(t)$ is the vector of orthogonal phase voltages which in the particular case of balanced conditions equals to:

$$v^{\perp}(t) = \frac{1}{\sqrt{3}} [v_b - v_c, v_c - v_a, v_a - v_b] \quad (10)$$

The instantaneous active and reactive powers of phase $m = \{a, b, c\}$ can be formulated as:

$$p_m(t) = v_m(t) \cdot i_m(t) \quad q_m(t) = v^{\perp}_m(t) \cdot i_m(t) \quad (11)$$

These power components can be divided into constant and variable terms as they depend on the product of two sinusoidal magnitudes,

$$p_m(t) = \overline{p}_m + \widetilde{p}_m(t) \quad q_m(t) = \overline{q}_m + \widetilde{q}_m(t) \quad (12)$$

where $\overline{p}_m$ and $\overline{q}_m$ refer to the constant terms and $\widetilde{p}_m(t)$ and $\widetilde{q}_m(t)$ to the oscillatory ones of the phase $m = \{a, b, c\}$.

These instantaneous power components can be used as setpoints for the real-time control of the VSC since the current references can be computed given the VSC output voltages. With this regard, it is worth noting that the steady-state condition of loads/generators are defined just with the terms $\overline{p}_m$ and $\overline{q}_m$ in (12). The oscillatory terms $\widetilde{p}_m(t)$ and $\widetilde{q}_m(t)$ remain undefined and, therefore, it is not straightforward to set the instantaneous power components required for the real-time control of the VSC.

REFERENCES

[1] IEEE PES AMPS DSAS Test Feeder Working Group (https://cmte.ieee.org/pes-testfeeders/resources/)

[2] CIGRE Task Force C6.04.02, Benchmark systems for network integration of renewable and distributed energy resources. Technical Brochure 575, 2014.

[3] EPRI Test Circuits https://sourceforge.net/p/electricdss/code/HEAD/tree/trunk/Distrib/EPRITestCircuits/

[4] V. Rigoni, L. F. Ochoa, G. Chicco, A. Navarro-Espinosa and T. Gozel, "Representative residential LV feeders: A case study for the North West of England", IEEE Trans. on Power Systems, Vol. 31, No. 1, pp. 348-360, January 2016.

[5] J. Dickert, M. Domagk and P. Schegner, "Benchmark low voltage distribution networks based on cluster analysis of actual grid properties", 2013 IEEE Grenoble Conference, 2013, pp. 1-6.

[6] K.P. Schneider, Y. Chen, D.P. Chassin, R.G. Pratt, D.W. Engel, S.E. Thompson, "Modern Grid Initiative Distribution Taxonomy Final Report", Pacific Northwest National Lab, 2008, doi:10.2172/104068.

[7] A. Koirala, L. Suárez-Ramón, B. Mohamed, P. Arboleya, "Non-synthetic European low voltage test system", International Journal of Electrical Power & Energy Systems, Vol. 118, 2020, 105712.

[8] H. Ahmad and M. I. Jambak, "Advanced laboratory scale model of high phase conversion power transmission line," 2008 IEEE 2nd International Power and Energy Conference, 2008, pp. 822-827.

[9] A. Ahlawat and S. T. Nagarajan, "Laboratory Scale Power Cable Model For Power System Education," 2020 International Conference for Emerging Technology (INCET), 2020, pp. 1-5.

[10] K.K. Challa, G. Gurrala, "Development of an Experimental Scaled-Down Frequency Dependent Transmission Line Model", IEEE Access, vol. 9, pp. 64639-64652, 2021.

[11] G. Gurrala, K. K. Challa and K. B. Rajesh, "Development of a Generalized Scaled-Down Realistic Substation Laboratory Model for Smart Grid Research and Education," in IEEE Access, vol. 10, pp. 5424-5439, 2022.

[12] Y. Noda, T. Mizuno, H. Koizumi, K. Nagasaka, K. Kurokawa, "The development of a scaled-down simulator for distribution grids and its application for verifying interference behavior among a number of module integrated converters (MIC)", Conference Record of the Twenty-Ninth IEEE Photovoltaic Specialists Conference, pp. 1545-1548, 2002.

[13] Y. Liu, C. Farnell, K. George, H. A. Mantooth and J. C. Balda, "A scaled-down microgrid laboratory testbed," 2015 IEEE Energy Conversion Congress and Exposition (ECCE), 2015, pp. 1184-1189.

[14] F. Huerta, J. K. Gruber, M. Prodanovic, P. Matatagui, T. Gafurov, "A laboratory environment for real-time testing of energy management scenarios: Smart Energy Integration Lab (SEIL)", 2014 International Conference on Renewable Energy Research and Application (ICRERA), pp. 514-519, 2014.

[15] A. Recalde, S. Bozhko, J. Atkin and S. Sumsurroah, "A Direct Current Power System Testbed for a More Electric Aircraft Application," 2021 AIAA/IEEE Electric Aircraft Technologies Symposium (EATS), pp. 1-15.

[16] C. Orozco-Henao, J. Marín-Quintero, R. Castillo-Sierra, J.C. Velez, I. Oliveros, M. Pardo, "Active Distribution Networks Laboratory: A Case of Experiments in Power Quality", 2019 IEEE Workshop on Power Electronics and Power Quality Applications (PEPQA), pp. 1-6, 2019.

[17] J. Tang, B. Xiong, C. Yang, C. Tang, Y. Li, G. Su, X. Bian, "Development of an Integrated Power Distribution System Laboratory Platform Using Modular Miniature Physical Elements: A Case Study of Fault Location", Energies, vol. 12, 3780, 2019.

[18] C. Yang, J. Tang, F. Zhang, D. Yang, T. Wu and W. Qi, "Development and Experimental Validation of Scaled-Down Analogous Power Distribution System with Single-Phase Arc Fault Generator," 2020 International Conference on Smart Grids and Energy Systems (SGES), 2020, pp. 49-54.

[19] J.M. Maza-Ortega, M. Barragán-Villarejo, F.P. García-López, J. Jiménez, L. Alvarado-Barrios, A. Gómez-Expósito, "A Multi-Platform Lab for Teaching and Research in Active Distribution Networks", IEEE Trans. on Power Systems, vol. 32, no. 6, pp. 4861-4870, Nov. 2017.

[20] B. P. Bhattarai, M. Lévesque, M. Maier, B. Bak-Jensen and J. Radhakrishna Pillai, "Optimizing Electric Vehicle Coordination Over a Heterogeneous Mesh Network in a Scaled-Down Smart Grid Testbed," in IEEE Transactions on Smart Grid, vol. 6, no. 2, pp. 784-794, March 2015.

[21] A. Das, E. I. Batzelis, S. Anand and S. R. Sahoo, "Network-Agnostic Adaptive PQ Adjustment Control for Grid Voltage Regulation in PV Systems," in IEEE Transactions on Industry Applications, vol. 58, no. 5, pp. 5792-5804, Sept.-Oct. 2022.

[22] F.P. García-López, M. Barragán-Villarejo, A. Marano-Marcolini, J.M. Maza-Ortega, J.L. Martínez-Ramos, "Experimental Assessment of a Centralised Controller for High-RES Active Distribution Networks", Energies, vol. 11, 3364, 2018.

[23] G. Kryonidis, M. Barragán-Villarejo, F.P. García-López, K.M. Malamaki, J.M. Mauricio, J.M. Maza-Ortega, C. Demoulias, "Experimental Validation of A Rule-Based Voltage Regulation Algorithm For Mv Grids", IEEE Powertech, Belgrade, 2023.

[24] H.L. Willis, "Power Distribution Planning Reference Book", 2nd ed.; CRC Press: Boca Raton, FL, USA, March 2004; ISBN 978-0824748753

[25] B. Lacroix and R. Calvas, "Earthings systems worldwide and evolution",Schneider electric –Cahier Technique no. 173

[26] GHOSHAL, A. N.I.R.B.A.N. and JOHN, V. I.N.O.D., "A controller design method for 3 phase 4 wire grid connected VSI with LCL filter," in Sadhana - Academy Proceedings in Engineering Sciences, vol. 40, no. 5, pp. 1481-1499, 2015

[27] Peng, F. Z., & Lai, J. S., "Generalized instantaneous reactive power theory for three-phase power systems," in IEEE Transactions on Instrumentation and Measurement, vol. 45, no. 1, pp. 293–297, 1996

[28] A. Yazdani and R. Iravani, *Voltage-Sourced Converters in Power Systems: Modeling, Control, and Applications*. Hoboken, NJ, USA: Wiley, 2010.

[29] W.H. Kersting, "Distribution System Modeling and Analysis", 3rd ed.; CRC Press: Boca Raton, FL, USA,February 2016

[30] F. Olivier, R. Fonteneau and D. Ernst, "Modelling of three-phase four-wire low-voltage cables taking into account the neutral connection to the

earth", CIRED Workshop on Microgrids and Local Energy Communities, Ljubljana, 7-8 June 2018 Paper 0593
[31] W. H. Kersting and W. H. Phillips, "Distribution feeder line models," in IEEE Transactions on Industry Applications, vol. 31, no. 4, pp. 715-720, July-Aug. 1995
[32] J. Xu, H. Qian, S. Bian, Y. Hu, and S. Xie, "Comparative study of single- phase phase-locked loops for grid-connected inverters under non-ideal grid conditions," CSEE Journal of Power and Energy Systems, vol. 8, no. 1, pp. 155–164, 2022.
[33] L. Moreno-Díaz, E. Romero-Ramos, A. Gómez-Expósito, E. Cordero-Herrera, J. R. Rivero and J. S. Cifuentes, "Accuracy of Electrical Feeder Models for Distribution Systems Analysis," 2018 International Conference on Smart Energy Systems and Technologies (SEST), Seville, Spain, 2018, pp. 1-6

A.M. Gross-Muresan was born in Romania in 1991. He received his degree in electrical engineering and master degree from the University of Huelva in 2014 and 2017 respectively. He has been with the Department of Electrical Engineering of the University of Seville since 2018, where he is a Ph.D. student working as a Laboratory Technician. His main interests lie in management and control of scaled-down networks and digital control of grid-tied converters.

F.J. Matas-Díaz was born in Spain in 1995. He received the aerospace engineering degree and the Master degree in power systems from the University of Seville, Seville, Spain, in 2017 and 2020 respectively, where he is currently a research assistant at the Department of Electrical Engineering. His primary research interests involve the control of power converters and the provision of ancillary services related to power quality, as well as HIL testing and experimental validation of power converters.

M. Barragán-Villarejo was born in Marmolejo, Spain, in 1984. He received the degree in electrical engineering and the Ph.D. degree in electrical engineering from the University of Seville, Seville, Spain, in 2008 and 2014, respectively. Since 2008, he has been with the Department of Electrical Engineering, University of Seville, where he is currently an Associate Professor. His primary research interests include the exploitation and control of power converters for smart grid management and the grid integration of renewable energy resources.

J.M. Maza-Ortega (Member, IEEE) received the degree in electrical engineering and the Ph.D. degree from the University of Seville, Spain, in 1996 and 2001, respectively. Since 1997, he has been with the Department of Electrical Engineering, University of Seville, where he is currently a Professor. His research interests include power quality, the integration of renewable energy in the grid and power electronics applications to transmission and distribution systems.

E. Romero-Ramos received the Electrical Engineering and Ph.D. degrees from the University of Seville, Spain, in 1992 and 1999, respectively. Since 1993, she has been with the Department of Electrical Engineering, University of Seville, where she is currently a Professor. She is interested in state estimation, load flow problems, optimal power system operation and analysis, and control of active distribution systems.